Nanoantenna coupled UV subwavelength photodetectors based on GaN

Serkan Butun,[1,2,*] Neval A. Cinel,[1,3] and Ekmel Ozbay[1,2,3]

[1]*Nanotechnology Research Center, Bilkent University, Bilkent, 06800 Ankara, Turkey*
[2]*Department of Physics, Bilkent University, 06800 Ankara, Turkey*
[3]*Department of Electric and Electronics Engineering, Bilkent University, 06800 Ankara, Turkey*
[*]*butun@bilkent.edu.tr*

Abstract: The integration of nano structures with opto-electronic devices has many potential applications. It allows the coupling of more light into or out of the device while decreasing the size of the device itself. Such devices are reported in the VIS and NIR regions. However, making plasmonic structures for the UV region is still a challenge. Here, we report on a UV nano-antenna integrated metal semiconductor metal (MSM) photodetector based on GaN. We designed and fabricated Al grating structures. Well defined plasmonic resonances were measured in the reflectance spectra. Optimized grating structure integrated photodetectors exhibited more than sevenfold photocurrent enhancement. Finite difference time domain simulations revealed that both geometrical and plasmonic effects played role in photocurrent enhancement.

OCIS codes: (040.5160) Photodetectors; (040.7190) Ultraviolet; (250.5403) Plasmonics; (050.6624) Subwavelength structures.

References and links

1. E. Ozbay, "Plasmonics: merging photonics and electronics at nanoscale dimensions," Science **311**(5758), 189–193 (2006).
2. A. Akbari and P. Berini, "Schottky contact surface-plasmon detector integrated with an asymmetric metal stripe waveguide," Appl. Phys. Lett. **95**(2), 021104 (2009).
3. A. Akbari, R. N. Tait, and P. Berini, "Surface plasmon waveguide Schottky detector," Opt. Express **18**(8), 8505–8514 (2010).
4. S. Collin, F. Pardo, R. Teissier, and J.-L. Pelouard, "Efficient light absorption in metal–semiconductor–metal nanostructures," Appl. Phys. Lett. **85**(2), 194–196 (2004).
5. T. Ishi, J. Fujikata, K. Makita, T. Baba, and K. Ohashi, "Si nano-photodiode with a surface plasmon antenna," Jpn. J. Appl. Phys. **44**(12), L364–L366 (2005).
6. J. A. Shackleford, R. Grote, M. Currie, J. E. Spanier, and B. Nabet, "Integrated plasmonic lens photodetector," Appl. Phys. Lett. **94**(8), 083501 (2009).
7. C. L. Tan, V. V. Lysak, K. Alameh, and Y. T. Lee, "Absorption enhancement of 980 nm MSM photodetector with a plasmonic grating structure," Opt. Commun. **283**(9), 1763–1767 (2010).
8. J. S. White, G. Veronis, Z. Yu, E. S. Barnard, A. Chandran, S. Fan, and M. L. Brongersma, "Extraordinary optical absorption through subwavelength slits," Opt. Lett. **34**(5), 686–688 (2009).
9. Q. Q. Gan, L. C. Zhou, V. Dierolf, and F. J. Bartoli, "UV plasmonic structures: direct observations of UV extraordinary optical transmission and localized field enhancement through nanoslits," IEEE Photon. J. **1**(4), 245–253 (2009).
10. Q. Q. Gan, L. C. Zhou, V. Dierolf, F. J. Bartoli, and Ieee, "UV extraordinary optical transmission through nanoslits," in Proceedings of the 2009 IEEE Leos Annual Meeting Conference, 1 and 2 (IEEE, New York, 2009), pp. 154–155.
11. J. Lin, A. Mohammadizia, A. Neogi, H. Morkoc, and M. Ohtsu, "Surface plasmon enhanced UV emission in AlGaN/GaN quantum well," Appl. Phys. Lett. **97**(22), 221104 (2010).
12. T. W. Ebbesen, H. J. Lezec, H. F. Ghaemi, T. Thio, and P. A. Wolff, "Extraordinary optical transmission through sub-wavelength hole arrays," Nature **391**(6668), 667–669 (1998).
13. H. F. Ghaemi, T. Thio, D. E. Grupp, T. W. Ebbesen, and H. J. Lezec, "Surface plasmons enhance optical transmission through subwavelength holes," Phys. Rev. B **58**(11), 6779–6782 (1998).

#159498 - $15.00 USD Received 5 Dec 2011; revised 13 Jan 2012; accepted 13 Jan 2012; published 20 Jan 2012

14. L. Martín-Moreno, F. J. García-Vidal, H. J. Lezec, K. M. Pellerin, T. Thio, J. B. Pendry, and T. W. Ebbesen, "Theory of extraordinary optical transmission through subwavelength hole arrays," Phys. Rev. Lett. **86**(6), 1114–1117 (2001).
15. V. Mikhailov, G. A. Wurtz, J. Elliott, P. Bayvel, and A. V. Zayats, "Dispersing light with surface plasmon polaritonic crystals," Phys. Rev. Lett. **99**(8), 083901 (2007).
16. E. Popov, M. Nevière, S. Enoch, and R. Reinisch, "Theory of light transmission through subwavelength periodic hole arrays," Phys. Rev. B **62**(23), 16100–16108 (2000).
17. H. Lezec and T. Thio, "Diffracted evanescent wave model for enhanced and suppressed optical transmission through subwavelength hole arrays," Opt. Express **12**(16), 3629–3651 (2004).
18. G. Gay, O. Alloschery, B. Viaris de Lesegno, C. O'Dwyer, J. Weiner, and H. J. Lezec, "The optical response of nanostructured surfaces and the composite diffracted evanescent wave model," Nat. Phys. **2**(4), 262–267 (2006).
19. F. Kalkum, G. Gay, O. Alloschery, J. Weiner, H. J. Lezec, Y. Xie, and M. Mansuripur, "Surface-wave interferometry on single subwavelength slit-groove structures fabricated on gold films," Opt. Express **15**(5), 2613–2621 (2007).
20. H. Liu and P. Lalanne, "Microscopic theory of the extraordinary optical transmission," Nature **452**(7188), 728–731 (2008).
21. J. Weiner, "The physics of light transmission through subwavelength apertures and aperture arrays," Rep. Prog. Phys. **72**(6), 064401 (2009).
22. F. J. Garcia-Vidal, L. Martin-Moreno, T. W. Ebbesen, and L. Kuipers, "Light passing through subwavelength apertures," Rev. Mod. Phys. **82**(1), 729–787 (2010).
23. H. Raether, *Surface Plasmons on Smooth and Rough Surfaces and on Gratings* (Springer, 1988).
24. E. D. Palik, *Handbook of Optical Constants of Solids* (Academic Press Inc., New York, 1985).
25. D. Brunner, H. Angerer, E. Bustarret, F. Freudenberg, R. Hopler, R. Dimitrov, O. Ambacher, and M. Stutzmann, "Optical constants of epitaxial AlGaN films and their temperature dependence," J. Appl. Phys. **82**(10), 5090–5096 (1997).
26. S. Butun, M. Gokkavas, H. B. Yu, and E. Ozbay, "Low dark current metal-semiconductor-metal photodiodes based on semi-insulating GaN," Appl. Phys. Lett. **89**(7), 073503 (2006).
27. H. Yu, M. K. Ozturk, S. Ozcelik, and E. Ozbay, "A study of semi-insulating GaN grown on AlN buffer/sapphire substrate by metalorganic chemical vapor deposition," J. Cryst. Growth **293**(2), 273–277 (2006).

1. Introduction

Light detection garners a great deal of interest for many applications such as, solar cells, communication, imaging etc. They all share one common component that somehow absorbs the electromagnetic energy i.e. photon, and converts it to some other form of quasi-particle (electron-hole pairs, or phonons) to be measured. Technological advancements have led to the miniaturization of all the components in electro-optic circuits in order to overcome space and sensitivity issues. The reduction of the absorption cross section is the main setback for the miniaturization of the volume of a photodetector. The integration of nano-structures with solid-state devices has opened a new way to incorporate light into integrated circuits [1]. A carefully designed nano-antenna positioned on top of a photodetector, which is smaller in size than the wavelength of the incident light, can be used to collect more photons. There are many experimental and computational examples reported for such devices from the near-IR to visible spectrum [2–8]. However, there is not many research reported on plasmonic structures in the UV region. The commonly used metals silver and gold cannot be used in the UV region, simply because they do not support surface plasmons in this spectral region, whereas aluminum has a much higher bulk plasma frequency (approx. 15 eV) and supports surface plasmons in UV. Therefore, a correct metal would be aluminum for UV plasmonics. An optically small UV photodetector has many potential applications such as data storage, all optical integrated circuits, and focal plane arrays. Extraordinary UV transmission through aluminum gratings [9, 10] and enhanced light emission from AlGaN/GaN quantum wells by surface plasmon resonance [11] have been reported. However, no plasmonic-structure integrated photodetector working in the UV is reported up to now.

The early works of Ebbesen *et al*. [12, 13] has attracted vast attraction to this so called extraordinary light transmission (EOT) problem. First explanations were stated that the surface plasmon polaritons (SPP) excited on both sides of the surface coupled with the waveguide modes of the apertures causing this effect [14–16]. Later, Lezec *et al*. showed that SPPs are not required for EOT [17]. In their approach, they showed that evanescent waves

#159498 - $15.00 USD Received 5 Dec 2011; revised 13 Jan 2012; accepted 13 Jan 2012; published 20 Jan 2012

which are launched by diffracted waves by sub-wavelength features couples to the wave-guiding modes of the apertures. Afterward Gay *et al.* proved that the effect of SPPs exceeded that of evanescent surface waves (ESW), in a distance far beyond ESW decay length [18, 19]. Lalanne *et al.* developed an SPP model to explain EOT phenomenon [20]. They conclude that, for near IR region, SPP model holds well but there exists an ESW contribution along with the SPPs as well. In addition they reported that when the metal conductivity increases SPP model becomes less accurate. The physical mechanism behind EOT is not yet fully understood is still open to discussion [21]. However it is known that both ESWs and SPPs are playing a role in EOT [22].

In this work, we designed and fabricated a nano-antenna on top of an optically small UV photodetector based on GaN. We characterized the nano-structures through the reflection measurements. We measured the photocurrent enhancement due to the nano-antenna.

2. Theory

2.1 Surface plasmon polaritons

The dispersion relation of the SPP excited with a grating is given as follows [23]:

$$k_x = k_0 \cdot \sin\theta \pm \frac{2\pi l}{\Lambda} = k_0 \sqrt{\frac{\varepsilon \cdot \varepsilon_d}{\varepsilon + \varepsilon_d}} \qquad l = 1, 2, ... \tag{1}$$

where k_x, θ, Λ, ε and ε_d are the horizontal component of the momentum of incident light with momentum k_0, incidence angle, grating period, the dielectric function of the metal and dielectric function of the surrounding medium (air), respectively. Here, an in-plane momentum component $2\pi l/\Lambda$ of the grating is required to match the momentum conservation condition. Note that incident light should be in TM mode in order to excite SPP [21]. The dispersion relation of SPPs on metal/air interfaces with a grating period Λ = 300 nm is calculated using Eq. (1). The dielectric constants of the metals are used from Palik [24]. The results are presented in Fig. 1(a). In addition, the propagation length of the surface plasmons on flat metal dielectric interface is given as [21]

$$L_i = \frac{1}{2k_x^{"}} \tag{2}$$

Where $k_x^{"}$ is the imaginary part of the surface plasmon wavenumber. Given the dielectric permittivity of the Al, we calculated the propagation length as 4.2 μm at 320 nm UV excitation. Accordingly, MSM contact width was chosen as 3 μm in order to be below this value. Note that, there is no separation between the slits and the gratings because the whole surfaces of the MSM contacts are decorated with gratings. Therefore waveguide modes of the slits can be excited via SPPs.

2.2 FDTD simulations

We performed finite-difference time-domain (FDTD) simulations by a commercial software package developed by Lumerical Inc. The material data of metals and GaN were taken from Palik [24] and Brunner *et.al* [25]. respectively. The mesh sizes were set to values less than or equal to λ/14, where λ is the source wavelength divided by the refractive index of material of interest. The boundary conditions were set as perfectly matched layer (PML) in order to eliminate undesired reflections from boundaries. The simulation software ensures numerical stability by setting the time step less than 0.02 fs based on the chosen mesh sizes. The total absorbed light intensity is calculated by the integration of the E-field intensity over time and space. The enhancement in absorption is then determined by comparing the structure with and without the metal gratings for the TM mode. The Fig. 1(b) compares the abortion enhancement for the same grating/slit combination for various grating materials. We included

#159498 - $15.00 USD Received 5 Dec 2011; revised 13 Jan 2012; accepted 13 Jan 2012; published 20 Jan 2012

a hypothetical perfect electrical conductor (PEC) by setting the imaginary part of the dielectric permittivity to an exceptionally high value to evaluate the effect of geometrically excited ESWs. Figures 1(c) and 1(d) compares the total amount of absorbed light at a resonant (340 nm) and an off-resonant (280 nm) wavelengths, respectively.

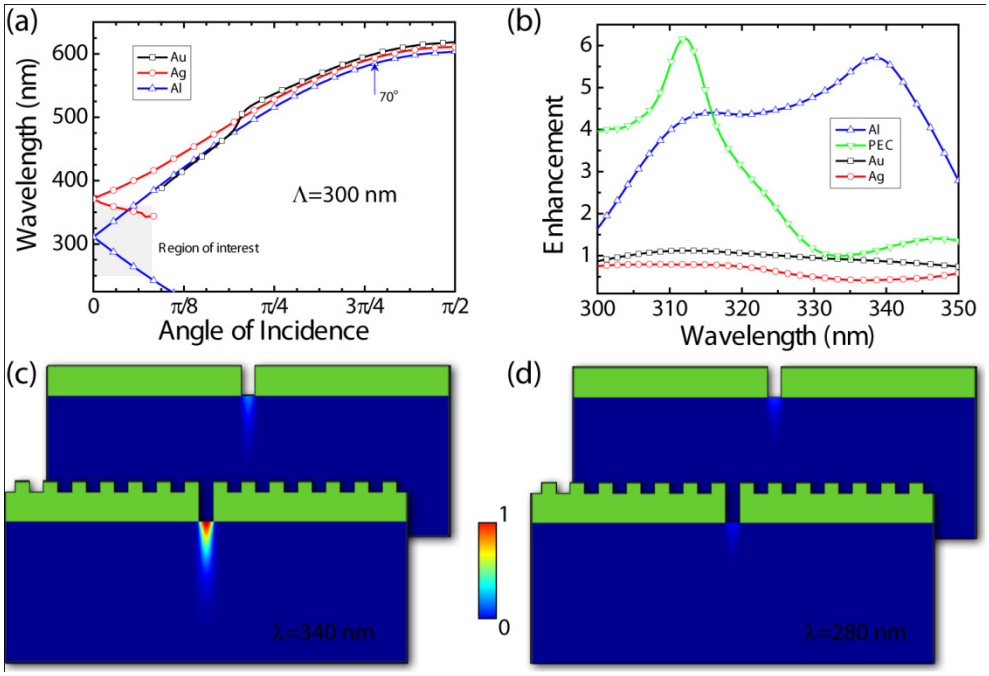

Fig. 1. Numerical simulations of the designed grating structures. (a) Calculated SPP dispersion relation of a grating/air interface for different metals. Here the grating period is 300 nm. The shaded region represents the absorption of GaN in vertical and the illumination cone of the lens in our setup in horizontal. (b) The spectral absorption enhancement results for different gating materials calculated by FDTD simulations. Simulation parameters were as follows; Slit width: 100 nm, base height: 75 nm and grove height: 35 nm. (c) and (d) are comparing the overall normalized E-field intensity under the slits with and without the gratings at a resonant and an off-resonant excitation. (The color bar applies to all)

3. Experiments

3.1 Fabrication

We used the so-called semi-insulating unintentionally doped GaN template for this work. Our previous research [26, 27] proved the superior quality of SI-GaN over the regular one in terms of leakage current. Especially GaN substrates with low leakage current characteristics were needed for the current work since the separation between the contact electrodes was very small. Therefore, the growth conditions were kept very similar to that reported in our previous works. The GaN epitaxial sample used in this study was grown on c plane sapphire in a cold wall low pressure MOCVD reactor. The Ga, Al, and N sources were Trimethylgallium (TMGa), trimethylaluminum (TMAl), and ammonia (NH_3), respectively, which were carried by hydrogen gas. The sapphire substrate was annealed at 1100 °C for 10 min for surface decontamination and cleaning, in the beginning. An essential 15 nm-thick AlN nucleation layer to compensate for the sapphire-AlN lattice mismatch was deposited at 840 °C. Consequently, the reactor temperature was gradually increased to 1,150 °C and an AlN buffer layer was grown. The growth was interrupted here to ensure the formation of abrupt AlN-GaN interface, meanwhile the growth conditions for GaN was achieved. An approximately 1 µm

#159498 - $15.00 USD Received 5 Dec 2011; revised 13 Jan 2012; accepted 13 Jan 2012; published 20 Jan 2012

thick GaN layer was grown under the following conditions: reactor pressure 200 mbar, growth temperature 1070 °C, and a growth rate of approx. 2 µm/h.

All the steps required for the fabrication of the plasmonic photodetectors were performed by electron beam lithography. We used polymethyl methacrylate (PMMA) as the e-beam resist and a two step lift-off process for the fabrication. The MSM contacts and the access pads were defined in the first step. The slit width between the contacts was optimized by varying the dose of e-beam exposure. The width of the contacts was 3 µm and the side size of each square in the photodetector was 150 µm. Then, the Ni/Al (10 nm/100 nm) metal pair was evaporated by e-beam evaporation. Ni was selected for its good Schottky contact characteristics on GaN, whereas Al was selected to maintain surface plasmon polaritons in the UV region because of its high plasma edge (15.2 eV). In the second step, gratings were written on a single part of the photodetector structure (see Fig. 2(a) and 2(b)). The actual sample grating period was 314 nm and duty cycle was 1/3. We evaporated 35 nm Al as grating metal.

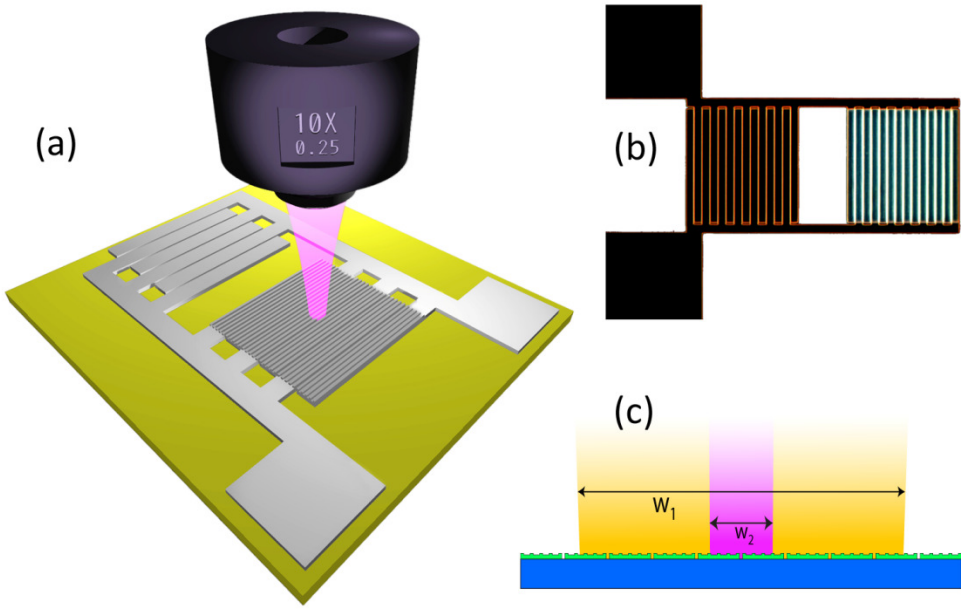

Fig. 2. Conceptual drawing of nano-structured MSM photodetector is given in (a). The lens that we used in the measurements is illustrated. (b) A dark field microscopy image of the fabricated photodetector. (c) A sketch illustrating the width of the illumination beam in spectral (w_1) and laser (w_2) measurements.

Optimization samples for reflection measurements were fabricated in the same manner on bare sapphire substrates. We prepared 300 × 300 μm^2 squares with the same slit spacing as on the device but various grating periods using the same metal type and thickness as described above. We also prepared slit samples without gratings for the reference measurements. (see Figs. 3(a) and 3(b))

3.2 Measurements

The reflection characteristics of the samples with various grating periods were carried out by ellipsometric measurements with Sentec 850 model ellipsometer equipped with a micro-spot adaptor. The measurement angle was 70°. Gratings were aligned such that they lie perpendicular to the plane of incidence. (TM mode) The reflected light was collected from

#159498 - $15.00 USD Received 5 Dec 2011; revised 13 Jan 2012; accepted 13 Jan 2012; published 20 Jan 2012

both samples with grating and reference samples, separately. Figure 3(c) presents the relative (wrt reference) spectral reflection data from three samples with different grating periods.

We measured the current-voltage (IV) characteristics of these devices in order to be sure that very closely separated MSM contacts (shown in detail in Fig. 4(a) and 4(b)) are in fact working properly. The results (Fig. 4(c)) indicated that, even if MSM contacts are as close as 150 nm they are well isolated from each other. The device break down voltage is measured around 15 V. That means the active GaN layer stands for electric field strength of over 1.0×10^6 V/cm. These values prove the good epitaxial and surface quality of our GaN material.

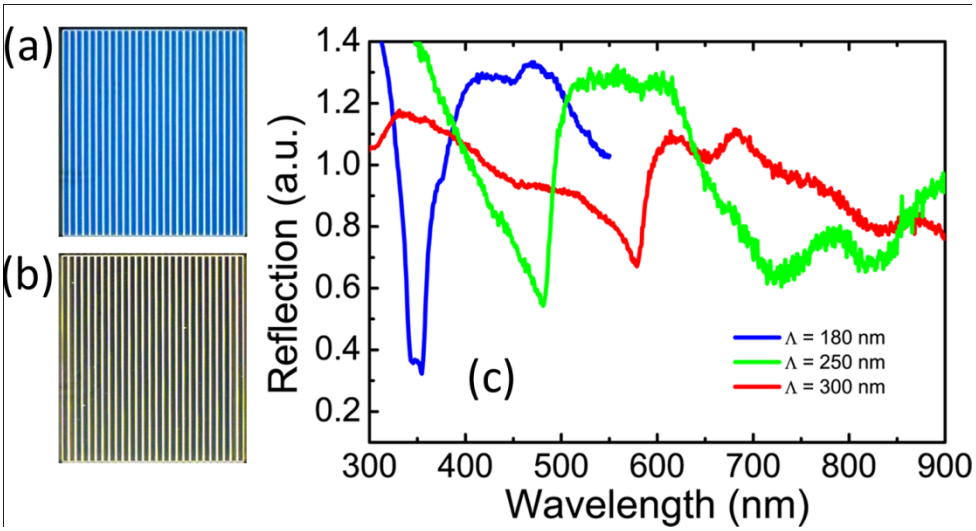

Fig. 3. Characterization of the plasmonic Al gratings fabricated on sapphire. (a) Spectral reflectance measurements of the Al gratings with different periods. (b) Dark-field microscopy image of a sample with grating period of 300 nm period. (c) Dark-field microscopy image of a sample without the grating. The data in (a) is obtained by dividing the reflection data of a grating by the data of the reference. Both the reference and the grating samples have slits.

Spectral device performance was characterized by a synchronous detection scheme. We illuminate the devices using a 10X UV objective with a numerical aperture of 0.25. The output of the Xe light source was monochromated and polarized, then coupled to the illumination objective. The incoming UV light is focused to a specific site on the photodetector with a spot size of 20 μm in diameter which is confined enough considering the device area is 150×150 μm^2. Light was mechanically chopped and the photocurrent was recorded with a lock-in amplifier. We measured the optical power at the end of the optical path using a calibrated Si photodetector, as well. First, one side of the device where there is no grating on the contacts was illuminated and then the spectral photocurrent was recorded. After that, the other side of the device where there is grating on the contacts was illuminated and again the spectral photocurrent was recorded. The photocurrent levels measured in this configuration were quite low. A slight non-uniformity in the device or substrate could induce uncertainty in the photocurrent. Therefore making the devices as close as possible was crucial. That is why we fabricated our devices in such a geometry rather than as two separate grating and reference devices. The measured spectral photocurrent data is compared in Fig. 4(d). The peak photocurrent value for illumination over the grating site is 24.5 pA, whereas it is 3.4 pA for illumination over the no grating site at zero volt bias. These values correspond to the responsivities of 1.7 mA/W and 0.2 mA/W, respectively. We further measured photocurrent under linearly polarized 325 nm wavelength He-Cd laser source, which has an optical power over 3 orders of magnitude higher than our spectral setup. The spot size in this case was about 3 μm in diameter. The spot sizes in two different set up is illustrated in Fig. 2(c) in a

#159498 - $15.00 USD Received 5 Dec 2011; revised 13 Jan 2012; accepted 13 Jan 2012; published 20 Jan 2012

comparative manner. Measured photocurrent in TM mode was 60 nA at the grating site, where as it was 9 nA at the reference site. The photocurrent in TE mode was 9 nA and 8 nA for grating site and the reference site, respectively.

4. Results and discussion

The numerical simulations revealed that neither Au nor Ag could be used for photocurrent enhancement in UV photodetectors (Fig. 1(b)). The first reason is that they do not support SPPs in this region due to their permittivity. If we refer to the dispersion curves (Fig. 2(a)) of these metals there are no available modes in the region (shaded area) where GaN has absorption. Moreover, the sub-wavelength groves are effectively invisible to the incident wave. Therefore, they cannot excite evanescent waves on the surface. On the other hand the PEC curve proves that the geometrical excitation of the evanescent waves plays an important role in the enhancement. However, when we compare this to the Aluminum we conclude that the spectral behavior of the absorption changes significantly. This proves the role of SPPs in the process. However, the dominant mechanism behind the enhanced absorption is still unclear which is beyond the scope of this work. In addition, the E-filed intensity profiles of the Al gratings on GaN are provided in Fig. 1(c) and 1(d) for further visualization of the enhanced transmission at different wavelengths. We have a clear enhancement in the intensity where the wavelength is close to the resonance whereas there is not much transmission at an off resonant wavelength.

The dips in the reflection spectra as shown in Fig. 3(c) are due to coupling to SPPs, which are red shifted as the grating period increases. The calculated dispersion relation presented in Fig. 1(a) confirms this coupling. The resonance for an incidence angle of 70° is around 585 nm, which is in good agreement with the measured value (red curve in Fig. 3(c)). Our setup limits the angle of incidence. However, the dispersion relation (Fig. 1(a)) states that if we illuminated at a steeper angle the resonance would shift towards the UV where GaN has high absorption. Dark field microscopy images of the samples are shown in Fig. 3(a) with the grating (Λ = 300 nm), and in Fig. 3(b) without the grating. The light hits the sample at a very shallow angle due to the nature of the dark-field microscopy. The red curve in the reflectance spectra (Fig. 3(c)) asserts that red portion (around 550 to 650 nm) in the incident light is coupled to the surface plasmons. A bluish part of the incident light was then reflected from the grating sample. The reference sample, on the other hand, appears dark because there no specific wavelength dependence in the reflectance spectra.

The comparison of the spectral photocurrents presented in Fig. 4(d) is given in Fig. 4(e). There is an enhancement factor of about 8 at 322 nm in terms of responsivity. Our single wavelength excitation measurements are in agreement with the spectral measurements The FDTD simulations support the measured results, as well. The slight mismatch in the peak of the enhancement curves (experimental vs. simulation) can be attributed to the poor parameter fitting of the simulation software to the inadequate GaN material data towards the absorption edge of the material.

#159498 - $15.00 USD Received 5 Dec 2011; revised 13 Jan 2012; accepted 13 Jan 2012; published 20 Jan 2012

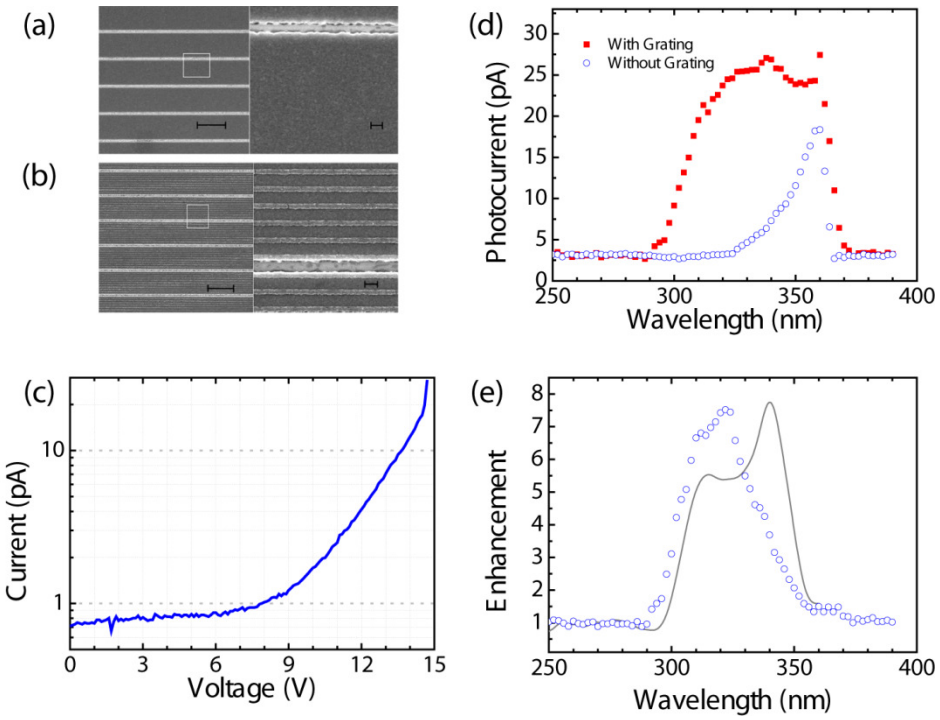

Fig. 4. Scanning electron microscopy images of the interdigitated MSM contacts (a) without the grating and (b) with the grating fabricated on top are shown. The longer and the shorter scale bars indicate 3 μm and 200 nm respectively. The measured dark current-voltage characteristics and the measured spectral photocurrent comparison are displayed in (c) and (d) respectively. The corresponding spectral enhancement is shown in (e). The dots are measurements and the solid line is the FDTD simulations of the fabricated device.

5. Conclusions

We successfully demonstrated an UV photodetector with a nano antenna. Plasmonic resonance of the designed antenna was determined from spectral reflectivity measurements. Then, we integrated this structure with a GaN UV photodetector. The electrical characterization indicated that the devices break down voltage was 15 V. The leakage current remained below 1 pA up to 7 V bias, even though the MSM contacts were placed 150 nm apart. The responsivity values were 1.7 mA/W and 0.2 mA/W at 322 nm UV illumination. The measured enhancement in photocurrent was eightfold. Numerical simulations revealed that this enhancement is both due to the geometrically excited evanescent waves as well as the SPPs. The experimental measurements and the numerical calculations were in good agreement.

Acknowledgments

The authors gratefully acknowledges the fruitful discussions with Mr. Atilla Özgür Çakmak This work is supported by the projects DPT-HAMIT, ESF-EPIGRAT, EU-N4E, NATO-SET-181 and TUBITAK under Project Nos., 107A004, 107A012, 109E301. One of the authors (E.O.) also acknowledges partial support from the Turkish Academy of Sciences.

#159498 - $15.00 USD Received 5 Dec 2011; revised 13 Jan 2012; accepted 13 Jan 2012; published 20 Jan 2012